

# Stable-V2A: Synthesis of Synchronized Sound Effects with Temporal and Semantic Controls

Riccardo Fosco Gramaccioni\*, Christian Marinoni\*, Emilian Postolache, Marco Comunità, Luca Cosmo, Joshua D. Reiss, Danilo Comminiello, *Senior Member, IEEE*

**Abstract**—Sound designers and Foley artists usually sonorize a scene, such as from a movie or video game, by manually annotating and sonorizing each action in the video. In our case, the intent is to leave full creative control to sound designers with a tool that allows them to bypass the more repetitive parts of their work, thus being able to focus on the creative aspects of sound production. We achieve this presenting Stable-V2A, a two-stage model consisting of: an RMS-Mapper that estimates an envelope representative of the audio characteristics associated with the input video; and Stable-Foley, a diffusion model based on Stable Audio Open that generates audio semantically and temporally aligned with the target video. Temporal alignment is guaranteed by the use of the envelope as a ControlNet input, while semantic alignment is achieved through the use of sound representations chosen by the designer as cross-attention conditioning of the diffusion process. We train and test our model on *Greatest Hits*, a dataset commonly used to evaluate V2A models. In addition, to test our model on a case study of interest, we introduce *Walking The Maps*, a dataset of videos extracted from video games depicting animated characters walking in different locations. Samples and code available on our demo page at <https://ispamm.github.io/Stable-V2A>.

**Index Terms**—video-to-audio, sound effects synthesis, diffusion models, audio-video synchronization, multimodal audio synthesis.

## I. INTRODUCTION

**S**OUND plays a key role in audiovisual storytelling. A scene, whether from a movie, video game, or any other kind of audiovisual media, can acquire completely different meanings depending on how it is sonorized. To do so, Foley artists and sound designers meticulously research sounds that can provide the right emotional impact to the audience; as an example we can consider the difference that may exist in the footstep sounds in a horror movie, where a certain degree of suspense is required, and a comedy. This means that creatives must choose the desired sound to be used for the scene and then manually annotate all occurrences of the action to be sonorized. Such mechanical action can be time-consuming, not allowing the artist to focus on the most important part of audiovisual narration: the choice and processing of sounds.

\*Equal contribution.

Riccardo Fosco Gramaccioni, Christian Marinoni and Danilo Comminiello are with the Dept. Information Engineering, Electronics and Telecommunications (DIET), Sapienza University of Rome, Italy. Marco Comunità and Joshua D. Reiss are with the Centre for Digital Music, Queen Mary University of London, UK. Emilian Postolache and Luca Cosmo are with the Dept. of Environmental Sciences, Informatics and Statistics, Ca' Foscari University of Venice, Italy.

Work done during Riccardo Fosco Gramaccioni's visiting period at Centre for Digital Music, Queen Mary University of London, UK.

Corresponding author's email: [riccardofosco.gramaccioni@uniroma1.it](mailto:riccardofosco.gramaccioni@uniroma1.it).

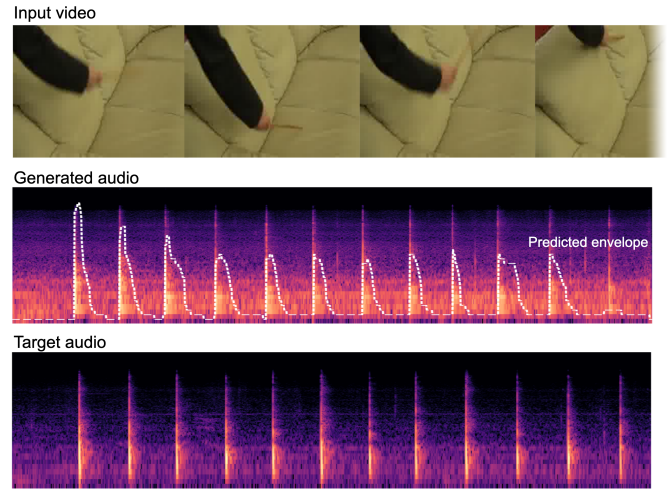


Fig. 1. Example showing ground truth audio and video, predicted RMS envelope and generated audio.

Thanks to the latest advancements in deep learning and the flourishing of multimodal generative models [1]–[3] and LLMs [4], [5], research in the audio field is getting increasing attention, as it is now feasible to control sound generation through different modalities not strictly related to audio signal processing, such as text [6]–[10]. Many recent research papers have focused on developing models for the generation of sounds that can be used as a soundtrack for video or images, opening up a new branch of research in the audio field, commonly referred to as Video-to-Audio [11]–[15].

The definition of a Video-to-Audio (V2A) task refers to a whole class of problems dealing with the generation of audio that is semantically and temporally aligned with a reference input video. Early research work in this area focused on developing deep learning models that could generate an audio that is only semantically aligned with an input image [13], [16], [17] or video [12], [18]. The intent in these cases is to generate a soundtrack for the scene that would highlight its overall mood [19], [20]. Models of this kind can successfully generate musical accompaniment and ambient sounds [21], [22] that can be used as background track. However, when specific actions, such as footsteps or the clapping of hands, are to be sonorized, a precise temporal alignment is required in order to give the scene all the realism it needs: it only takes a few milliseconds of asynchronism between the reference video and the audio for the audience to perceive a feeling

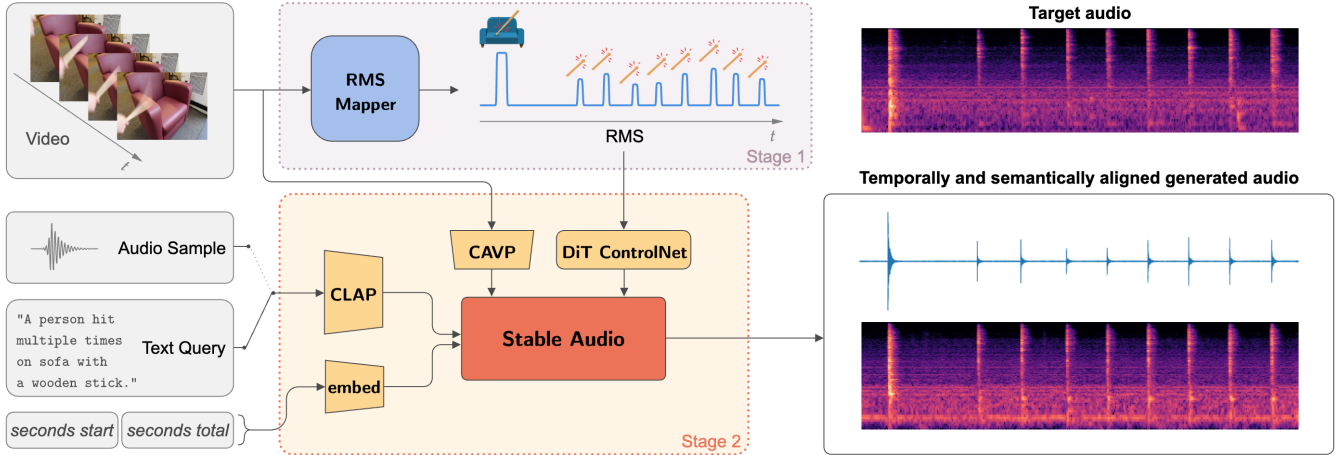


Fig. 2. Stable-V2A architecture consists of two distinct parts: RMS-Mapper, that predicts an envelope representative for the audio directly from the input video, and Stable-Foley, the audio synthesis model for the controlled generation of the final audio effect. The generation is controlled temporally by the predicted RMS envelope through a DiT ControlNet, and semantically by CLAP and CAVP embeddings. The length of the output waveform can be controlled with `seconds_start` and `seconds_total` parameters.

of estrangement [23].

Many papers that have attempted to achieve temporal as well as semantic alignment have focused on the design of end-to-end models that directly take as input the video to be sonorized and output the audio track related to that video [12], [15], [24]–[27]. Those models have shown remarkable results in V2A tasks but do not allow sound designers or Foley artists to have direct control over the audio generation process, other than being able to directly operate on the final output of the model. Other works, however, have approached the problem by dividing it into two distinct components: a model for extracting audio-relevant features from the video and an audio model that using those features, generates the audio of interest [28], [29]. Our model is a two-stage model as well. In fact, as in our previous work [30], we aim to use a video model to extract human-readable features from the video that are representative of the audio to be generated; in this paper, such features are represented by the envelope, as the envelope has proven to be an excellent control for the temporal alignment [31].

We do so because our intent is to provide creatives with the ability to control the generation process. For example, the sound designer might decide to make some sounds more intense than normal or add other sounds that are not directly visible, such as the case where a person’s footsteps precede their visual presence on the scene. In this way, by extracting a feature like the envelope from a video, the sound designer can directly edit this envelope to his convenience, before using it as a control for generating the final audio track.

Here we introduce a new two-stage model for V2A generation, **Stable-V2A**, where the two stages are represented by RMS-Mapper and Stable-Foley. The architecture of our complete model is shown in Fig. 2

**RMS-Mapper** is a simple but effective network for mapping an RMS envelope directly from a video; it takes representative features of frames and optical flow of videos as input. We use a widely employed video encoder for audiovisual tasks

[32] as baseline. The output is a curve that aims to replicate the RMS envelope, in terms of time alignment, time-varying intensity, and duration of each sound present in the target audio.

**Stable-Foley**, the model for synthesizing sound effects, relies on Stable Audio [33], a state-of-the-art latent diffusion model for audio generation, to obtain the final output. In order to take advantage of the prior knowledge of this model and guide its generation process via the RMS envelope, we leverage a ControlNet [34], which is a network used to control the diffusion process via extra conditioning.

Fig. 1 depicts an audio generated by Stable-Foley through the RMS-envelope predicted from RMS-Mapper.

The semantics of the final audio is specified by conditioning Stable-Foley with a latent representation of the audio sample representing the sound of the action in the video. This representation is obtained through CLAP [35], a state-of-the-art audio encoder based on contrastive learning, that aligns audio and textual modalities. Therefore, the desired timbre for the final audio track can be specified to the model either with a reference audio sample as well as with a textual description of the sound, also allowing for text-to-audio generation. Our model generates 44.1 kHz stereo audio of variable length.

We evaluate the proposed method on several objective metrics by training and testing the model on *Greatest Hits* [36], a dataset widely used to validate V2A models, consisting of videos of people hitting or scratching objects with a drumstick.

Finally, to test the model on a case study of interest, which is the generation of footstep sounds [37], we introduce a dataset of videos extracted from video games session containing animated characters walking in different environments, called *Walking The Maps*. The videos are taken from YouTube and selected in order to have as few background noises as possible, so that the audio of each video contains mainly the sound of footsteps.

Thus, our contributions can be summarized as follows:

- We present Stable-V2A, a two-stage model for generating audio that is temporally and semantically aligned with a reference input video. Sound designers can control the generation of the final output through the use of an RMS envelope.
- We perform an evaluation through objective metrics that attest both temporal and semantic alignment capability of the model.
- We also introduce a brand-new dataset for the analysis of a case study of interest, which is the generation of footstep sounds, called *Walking The Maps*.

## II. RELATED WORKS

Generating audio that is aligned with a silent reference video is a problem of great interest today for multimedia post production. Due to recent developments in deep learning, many of the leading experts in the audiovisual industry are focusing their efforts on developing deep learning models that can be integrated into the principal post production tools [38]–[41].

Despite these advancements, generating audio from video still presents many challenges. Not only the audio produced must maintain semantic coherence with what is shown in the video, but generated sounds also have to exhibit enough time alignment with the actions throughout the video to allow an adequate sense of realism while watching the scene. Although several audio models manage to generate reasonably realistic sounds for Foley synthesis [31], [42]–[45], many V2A models struggle when it comes to actually achieving good time alignment.

Im2Wav [13] focuses on generating sounds that are semantically relevant to an image or sequence of images, using CLIP [46] to condition with visual features two transformer language models.

In order to perform a cross-modality generation between video and audio, Xing, et al. [47] propose a multimodality latent aligner with the pre-trained ImageBind [48] model, used to condition a latent diffusion model (LDM) in order to generate an audio that is semantically relevant for an input video.

RegNet [32] represents one of the first attempts to achieve semantic as well as temporal alignment. This model uses a simple and efficient video encoder that extracts relevant visual features from the frames and optical flow of an input video and uses them to condition a Generative Adversarial Network (GAN) to generate visually aligned sounds. SpecVQGAN [49] also uses RGB and optical flow features of a video but leveraging a more powerful Transformer-based autoregressive architecture to generate temporally and semantically aligned sounds to an input video.

A similar architecture is used in CondFoleyGen [50], where such a model is trained directly using *Greatest Hits*, succeeding in achieving an efficient alignment in both content and timing with the reference video. Instead, Diff-Foley [51] uses Contrastive Audio-Visual Pretraining (CAVP) to temporally and semantically align audio and video modalities, being able to generate a video embedding that contains features relevant

to the corresponding audio. Such features are used to directly condition an LDM.

However, all these models do not provide human-intelligible control, thus not allowing direct control by sound designers over the final generation, as they cannot act on either the semantics or the timing of the final output.

Our previous work, SyncFusion [30] - which was the first to introduce a human readable control for the V2A task - uses a video encoder based on a ResNet(2+1)D-18 [52] that, by taking frames of the target video as input, generates an onset track; this onset track is then passed to a time-domain diffusion model [53] to generate the final output. The visual representation provided by the onsets is very similar to the manual annotations used by sound designers when determining the temporal placements of the sound sources to be sonorized in a video. Therefore, it provides an informative and yet easy-to-edit control for the user, allowing direct oversight on the generation of the final output. This onset track is represented by a binary mask that indicates the presence or absence of the action of interest for each frame of the video. Hence, an onset can indicate the temporal location of a sound but can not inform either about the intensity or temporal duration.

Furthermore, the onset of a sound event cannot be determined unambiguously, as in the case of a sound event sustained over time where the temporal placement of the onset is not unequivocally determined. Consequently, in order to use onsets, it is necessary to have a dataset containing manually annotated onsets for every sound event in each video.

T-Foley [31], although not working with an input video, uses an envelope to condition a diffusion model similar to the one in SyncFusion, demonstrating the effectiveness of such a control for generating highly temporally conditioned audio. This model can generate sounds that follow with high accuracy the temporal guidance provided by the envelope, extending this idea in Video-Foley [54], where AudioLDM [6] is employed to generate 16 kHz mono audio aligned temporally and semantically with the input video.

## III. BACKGROUND

### A. Audio Diffusion Models

Diffusion Models currently represent the state-of-the art in generative deep learning. They are based on non-equilibrium thermodynamics and are defined by a Markov chain of diffusion steps that slowly add noise to target data. The aim of such models is to reverse this process in order to learn how to generate data of interest from noise.

Denosing Diffusion Probabilistic Models were introduced in [55]. They were first used to obtain state-of-the-art results in image generation and then in the generation of other kind of data, such as video and audio.

Like Diffusion Models for images, Audio Diffusion Models (ADM) start by producing a random, noisy audio signal and gradually enhance it through multiple refining iterative steps. In each step, the noise is reduced, and finer details are added to the audio. Such models have been used to generate both music [56] and environmental sounds [57].

Latent Diffusion Models [58] perform the diffusion process in the latent space. In this case, high-dimensional data of

interest  $\mathbf{y}$ , such as audio, are encoded in low-dimensional latent embeddings  $\mathbf{z} = \mathcal{E}(\mathbf{y})$ , providing a more meaningful representation for training the network. For V2A, the process is guided by a set of conditionings  $\mathbf{C} = \mathbf{c}_1, \mathbf{c}_2, \dots, \mathbf{c}_n$ . In the forward process, Gaussian noise is slowly added to the original data distribution with a fixed schedule  $\alpha_1, \dots, \alpha_T$ , where  $T$  is the total timesteps, and  $\bar{\alpha}_t = \prod_{i=1}^t \alpha_i$ :

$$q(\mathbf{z}_t | \mathbf{z}_{t-1}) = \mathcal{N}(\mathbf{z}_t; \sqrt{\alpha_t} \mathbf{z}_{t-1}, (1 - \alpha_t) \mathbf{I}) \quad (1)$$

$$q(\mathbf{z}_t | \mathbf{z}_0) = \mathcal{N}(\mathbf{z}_t; \sqrt{\bar{\alpha}_t} \mathbf{z}_0, (1 - \bar{\alpha}_t) \mathbf{I}). \quad (2)$$

The model should attempt to reverse the process by optimizing a denoising objective, typically defined as:

$$\mathcal{L}_{\text{LDM}} = \mathbb{E}_{\mathbf{z}_0, t, \epsilon} \|\epsilon - \epsilon_\theta(\mathbf{z}_t, t, \mathbf{C})\|_2^2, \quad (3)$$

where  $\epsilon$  is Gaussian noise and  $\epsilon_\theta(\mathbf{z}_t, t, \mathbf{C})$  denotes the estimated noise, which is the output of the model.

After training, LDMs generate latents by sampling through the reverse process with  $\mathbf{z}_T \sim \mathcal{N}(0, \mathbf{I})$  formulated as:

$$p_\theta(\mathbf{z}_{t-1} | \mathbf{z}_t) = \mathcal{N}(\mathbf{z}_{t-1}; \mu_\theta(\mathbf{z}_t, t, \mathbf{C}), \sigma_t^2 \mathbf{I}) \quad (4)$$

$$\mu_\theta(\mathbf{z}_t, t, \mathbf{C}) = \frac{1}{\sqrt{\alpha_t}} \left( \mathbf{z}_t - \frac{1 - \alpha_t}{\sqrt{1 - \bar{\alpha}_t}} \epsilon_\theta(\mathbf{z}_t, t, \mathbf{C}) \right) \quad (5)$$

$$\sigma_t^2 = \frac{1 - \bar{\alpha}_{t-1}}{1 - \bar{\alpha}_t} (1 - \alpha_t). \quad (6)$$

Finally, the desired output  $\hat{\mathbf{y}}$  is obtained by decoding the generated latent  $\mathbf{z}_0$  with a decoder  $\mathcal{D}$ .

These models are widely used for audio generation [59], with Stable Audio [60], [61] representing a state-of-the-art latent ADM in generative deep learning for audio.

### B. Guiding diffusion processes with ControlNet

ControlNet [34] is a neural network specifically designed for diffusion models that allows for more precise control over the generation process by conditioning the model on additional inputs. It was first used to control image generation in Stable Diffusion with extra information such as features or prompts. Initially designed for U-Net-based diffusion models, ControlNet was later extended in [62] to work with Diffusion Transformers (DiT).

In audio diffusion models, ControlNet can guide the generation of sound by incorporating specific constraints like tempo, rhythm, pitch, or other audio characteristics [63]. This makes it useful for tasks like generating audio that adheres to a desired structure or style, improving the accuracy and flexibility of the diffusion process.

## IV. PROPOSED METHOD

### A. Problem Formulation

Let us consider a target video  $\mathbf{x} \in \mathbb{R}^{T \times C \times H \times W}$ , where  $T$  is the total duration of the video expressed in frames,  $C$  is the number of input RGB channels, i.e. 3 channels,  $H \times W$  is the dimension in height and width of each frame. The objective of the proposed model is to generate an audio track  $\mathbf{y} \in \mathbb{R}^{Ch \times L}$ , where  $Ch$  represents the number of audio channels, that is 2 for stereo audio, and  $L$  is the time duration of the audio expressed in samples. The generated audio  $\mathbf{y}$  must be semantically and temporally aligned to the input video, so it can be used as a realistic soundtrack for it. For example, in the case of a video depicting a person walking slowly on a wooden pavement, the audio generated by the model must be both in terms of semantics and temporal alignment distant from the audio generated for a video depicting a person running on grass.

One of the main challenges when approaching V2A problems is the completely different temporal resolution between video and audio. Indeed, the temporal resolution of a video, expressed in frames per second (*fps*), is usually much lower than the temporal resolution of an audio, expressed in sample rate (*sr*). For instance, a commonly used frame rate in video is 25 *fps*, while the standard in audio is represented by a *sr* of 44.1 kHz. This means that in this specific case 1764 audio samples are represented by one single frame. One possible solution is to increase the *fps* of the video and lower the *sr* of the audio, to mitigate that difference, as we partially do in our video model. However, increasing the frame rate of a video excessively leads to a significant rise in the computational cost of the model. On the other hand, decreasing the sample rate results in a loss of audio quality, which is unsuitable for practical use in sound design. It is therefore crucial to carefully manage the transition between the two modalities, i.e. audio and video, to ensure the problem remains computationally feasible while maintaining the audio quality necessary to capture all the sound features needed by sound designers and Foley artists [64], [65].

### B. Mapping a Video to an Envelope

In audio, the envelope describes how a sound evolves over time. It is represented by a smooth curve outlining the extremes of the signal, providing useful information such as its amplitude and duration over time. Moreover, by tracking the shape of the waveform, it is an effective and visually understandable feature for indicating the temporal locations of all sound events in the audio.

The envelope can be calculated in different manners. In T-Foley [31], the Root-Mean-Square (RMS) of the waveform, a commonly used frame-level amplitude envelope feature, is employed for temporal-event guided waveform generation. The  $i$ -th sample of the temporal sequence representing the RMS envelope is then calculated on a window of the audio signal  $\mathbf{y}$  as follows:

$$\mathbf{r}_i = \mathbf{RMS}_i(\mathbf{y}) = \sqrt{\frac{1}{W} \sum_{t=ih}^{ih+W} \mathbf{y}^2(t)}, \quad (7)$$

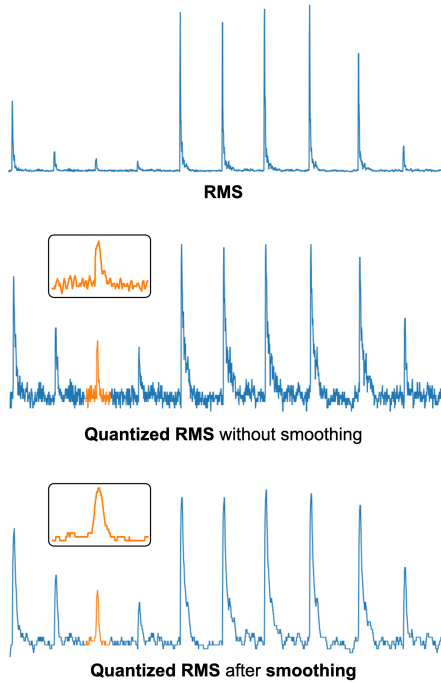


Fig. 3. Example of the ground truth envelope before and after the smoothing operation.

where  $W$  is the window size and  $h$  is the hop size.

Similarly to [54], we address this task as a classification one since trying to map a curve representing the envelope of an audio as a regression task does not produce satisfactory results. This is because sounds related to actions are often transient, which makes audio containing multiple repeated actions sparse, meaning that most samples represent silence. A model that tries to map such a time series as a regression task thus tends to predict silence or the mean value of the curve, as we also found out in our early experiments.

We then perform amplitude quantization of the envelope by  $\mu$ -law encoding. Such encoding is widely used in audio, especially in pitch estimation [66], precisely to mitigate the transient and sparse nature of waveform of this kind. The  $\mu$ -law encoding reduces the dynamic range of an audio signal and is formulated as follows:

$$\mu\text{-law}(\mathbf{r}) = \frac{\ln(1 + \mu|\mathbf{r}|)}{\ln(1 + \mu)} \cdot \text{sgn}(\mathbf{r}), \quad (8)$$

where  $\mathbf{r}$  is the RMS envelope of the target audio  $\mathbf{y}$ .

This encoding allows amplitude quantization of the signal by dividing the values into equidistant bins. The idea here is to map video frames to specific classes, representing the amplitude values of the envelope. This conceptually is very close to what we did in SyncFusion [30], by simply extending the binary classification task of an onset track to the multi-class classification task, where each class represents a given range of the continuous envelope amplitude values.

Furthermore, it is necessary not to penalize near-correct predictions. Indeed, a precise prediction of the correct class is desirable but not strictly required to ensure good perceptual

quality: by using 64 equidistant bins as classes, each would correspond to an amplitude resolution of 0.50 dB. Selecting a bin next to the true one would introduce an error that is barely perceptible.

Then, in order to minimize the penalty of a near-correct class prediction, Gaussian label smoothing on the target envelopes - as proposed in [67] - is used:

$$\mathbf{r}(i) = \begin{cases} \exp\left(-\frac{(c_i - c_{\text{gt}})^2}{2\sigma^2}\right) & \text{if } |c_i - c_{\text{gt}}| \leq W \text{ (} c_i, c_{\text{gt}} \neq 0 \text{)} \\ 0 & \text{otherwise,} \end{cases} \quad (9)$$

where  $i$  is the class index,  $c_{\text{gt}}$  is the ground-truth class,  $\sigma = 1$ , and  $W$  is the window size on whose values the smoothing is applied.

### C. Stage 1: RMS-Mapper

The first stage of our model, the RMS-Mapper, is a simple neural network that takes some features extracted from the video as input and generates a temporal guide for the sound synthesis process of Stage 2.

The target is an envelope extracted from a corresponding 10 seconds audio chunk sampled at 16 kHz. This relatively low sample rate helps reduce the temporal resolution gap between audio and video while preserving sufficient detail in the audio track. We compute the RMS with the function implemented in the Librosa Feature module<sup>1</sup>. Following the nomenclature of Eq. 7, we set  $W = 512$  and  $h = 128$ , thus obtaining an envelope  $\mathbf{r}$  with 1250 time samples. Since we normalize the audio  $\mathbf{y}$  in the  $[-1, 1]$  range, the resulting  $\mathbf{r}$  is a curve with values in the range  $[0, 1]$ .

In addition, to mitigate the high-frequency variations which are common in real sound waveforms, we apply a smoothing filter with a kernel size of 15. Our experiments show that incorporating such a filter significantly improves the results, simplifying the classification task that the network performs on the video frames, as can be seen in Fig. 3.

Finally, we map the time-continuous RMS-envelope to 64 distinct classes, by applying  $\mu$ -law encoding, as reported in Eq. 8, using the function provided in the Librosa library<sup>2</sup>. We then apply Gaussian label smoothing on the target discretized envelope.

RMS-Mapper takes as input features extracted from the videos. We first convert each video to 30 *fps*, doubling the frame rate compared to our previous work [30]. This means that a 10 seconds long video is represented by a sequence of 300 consecutive frames.

In addition, we compute the optical flow of each video using the RAFT [68] model. Experimentally, we have noticed that the information contained in the optical flow is crucial for inferring a relationship between the motion in the video and the corresponding sound.

We use TC-CLIP [69] to extract relevant features from the RGB frames and the optical flow. Temporally Contextualized CLIP (TC-CLIP) is a model for video understanding that leverages essential temporal information through global interactions

<sup>1</sup><https://librosa.org/doc/main/generated/librosa.feature.rms.html>

<sup>2</sup>[https://librosa.org/doc/main/generated/librosa.mu\\_compress.html](https://librosa.org/doc/main/generated/librosa.mu_compress.html)

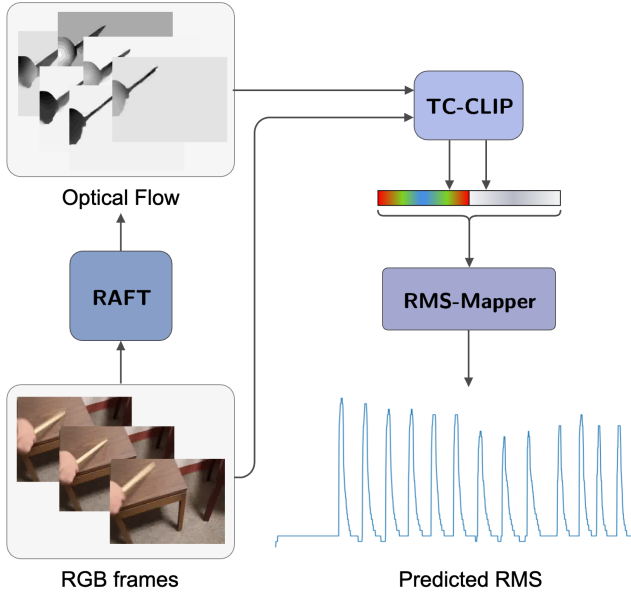


Fig. 4. Block diagram for the proposed RMS-Mapper.

in a spatio-temporal domain within a video. TC-CLIP generates 512 dimensional frame-wise features. We concatenate the RGB and optical flow features along the feature dimension, obtaining an input of size  $[\text{video\_frames}, 1024]$ , where in our case  $\text{video\_frames} = 300$  for *Greatest Hits* experiments.

Then, we use an efficient model based on the RegNet video encoder [32] to generate the output of our model. The network is composed of three 1D convolutional layers, a two-layer bidirectional LSTM (Bi-LSTM) [70] and a linear layer that projects the resulting features to the output size required for the classification task. We use the convolutional block as an upsample branch needed to scale features from video temporal resolution to the audio temporal resolution. Each convolutional layer is followed by a batch normalization layer, a ReLU activation function and an Upsample layer. The upsample sizes for the three layers are  $[600, 1200, 1250]$ , thus increasing the time dimension of the output from  $\text{video\_frames}$  to  $\text{RMS\_frames}$ , where  $\text{RMS\_frames}$  is equal to 1250. Thanks to this upsample, we do not perform a frame-by-frame classification of the video, but we directly map the continuous RMS envelope.

We use a Cross Entropy loss as objective for our classification problem:

$$\mathcal{L}_{\text{CE}}(\mathbf{r}_d, \hat{\mathbf{r}}_d) = - \sum_{i=1}^C \mathbf{r}_{d_i} \log(\hat{\mathbf{r}}_{d_i}), \quad (10)$$

where  $\mathbf{r}_d$  is the discretized RMS envelope  $\mathbf{r}$ , i.e. the envelope after  $\mu$ -law encoding and Gaussian label smoothing, and  $\hat{\mathbf{r}}_d$  is the output of our model. Fig. 4 depicts a block diagram of the proposed RMS-Mapper.

#### D. Stable-Foley

Stable-Foley is based on Stable Audio Open [33], which is an Audio Latent Diffusion Model for generating long-form, variable-length stereo music and sounds at 44.1 kHz using text

prompts. Therefore, this model is not specifically trained for V2A tasks, which means that the generated audio does not take into account a time alignment with a specific reference.

We want to use the prior knowledge of such a state-of-the-art model for audio synthesis, but at the same time guide audio generation both semantically and temporally. This means that the audio synthesis model should be controlled by the envelope extracted from the RMS-Mapper, representing our temporal control, and conditionings that capture the semantics and duration of the audio.

The aim of the synthesis model is to learn a probability distribution  $p(\mathbf{y}|\mathbf{F}, \mathbf{r})$  of a waveform  $\mathbf{y}$ , given a time-independent set of conditionings  $\mathbf{F} = \mathbf{f}_1, \mathbf{f}_2, \dots, \mathbf{f}_n$ , representing a set of  $n$  desired semantic characterizations, and  $\mathbf{r}$ , that is the temporal control.

Stable-Foley is trained on the same loss on which Stable Audio models are trained. As stated in [61], the final loss is the result of the combination of multiple losses: 1) a reconstruction loss based on a perceptually weighted multiresolution STFT [71]. This loss is computed on both the mid-side (M/S) and the left-right (L/R) representations of stereo audio. To address potential ambiguity in L/R channel placement, the L/R component is weighted at 0.5 relative to the M/S component. 2) an adversarial loss with feature matching incorporated, leveraging five convolutional discriminators [72]. 3) a KL divergence loss term with a weighting factor of  $10^{-4}$ .

1) *Temporal Control*: We use a ControlNet to drive generation using a temporal control and at the same time just fine-tune Stable Audio Open on our specific task, without having to train the model from scratch.

To the best of our knowledge, this is the first attempt to use a ControlNet to control the DiT generation process of Stable Audio with additional control. As ControlNet was originally developed for Diffusion U-Net, we followed what is done in [62] for our implementation of such network for Stable Audio.

We want to generate stereo audio at 44.1 kHz. In the training phase, the length of the audio to be generated is fixed at 10s. Accordingly we interpolate the ground truth RMS envelope, extracted for both L/R channels, to the length in samples of the target audio signal.

The input of the ControlNet needs to be of the same dimension as the input of the diffusion model, i.e. the embedding of the audio used in Stable Audio. To extract this latent representation of the envelope, we use the VAE introduced in [60] for encoding the input to the diffusion model, without needing to update its weights. This VAE downsamples the input stereo audio by a factor of 1024. Specifically, it maps an input signal  $\mathbf{y} \in \mathbb{R}^{2 \times L}$ , where  $L$  is the number of samples representing the waveform, and 2 is the number of channels, to an embedding  $\mathbf{y}_e \in \mathbb{R}^{64 \times \frac{L}{1024}}$ .

In all of our experiments, such a VAE has proven to provide a meaningful representation of the RMS envelope as well, so we use it to encode the input of the ControlNet  $\mathbf{r}$  and the diffusion process input  $\mathbf{y}$ .

For the design of Stable-Foley we follow the general architecture of ControlNet: the DiT layers are then frozen, and a trainable copy for each of them is created with two zero-initialized convolutional layers placed before and after the

copy. For training, the envelope is generated so that it has the same length in samples as the target audio. The control signal  $\mathbf{r}$ , representing the RMS envelope, and the input waveform  $\mathbf{y}$  are both encoded through the same VAE. For each layer, the encoded control signal  $\mathbf{r}_c$  is first processed through the initial zero-initialized convolutional layer, then added to the input  $\mathbf{y}_c$ , which is the latent version of  $\mathbf{y}$  obtained through the VAE; the resulting signal is subsequently passed through the trainable copy and the second zero-initialized convolutional layer and finally added to the output of the frozen layer, derived from input  $\mathbf{y}_c$ .

Finally, we use a `depth_factor` parameter to use only a subset of the pre-trained layers of the original DiT: in our experiments we use a `depth_factor` of 20%, which corresponds to using only 5 layers of the Stable Audio DiT.

2) *Semantic Control*: Lots of recent deep learning research has focused on developing versatile audio representations that can generalize effectively across various downstream tasks [73]. Contrastive learning, in particular, gained great popularity for the training of multimodal models. A notable example of this approach is CLAP [35], which aligns embeddings for both audio and text in a shared latent space. We then condition our sound synthesis model on CLAP audio embeddings during training, enabling it to incorporate text-based conditioning as an additional modality at inference time only.

To further refine the semantic and temporal alignment of the final audio, we also condition the generation process with a direct frame representation of the reference video. We do this using the latent representation provided by the CAVP video encoder, introduced in [51]. This video encoder aligns the audio and video modalities, providing useful information about the timing and semantics of the related audio. CAVP takes as input video at 4 *fps*, so we use this frame rate to pass only RGB frames to it.

These semantic controls are provided via cross-attention layers, as originally proposed for Stable Audio global conditionings.

Conditionings on duration, provided by the hyperparameters `seconds_start` and `seconds_total`, indicating the total length of the audio, are fed to the model via prepending it to the input of the model. Prepend conditioning includes also timestep conditioning, indicating the current diffusion timestep. Prepend conditionings are concatenated along the channels dimension to the input.

## V. EXPERIMENTAL SETUP

### A. Datasets

1) *Greatest Hits*: We use the *Greatest Hits* dataset [36], a widely-adopted datasets for V2A tasks. This dataset includes videos of humans using a drumstick to hit or rub objects or surfaces. The choice of a drumstick as the striking object is useful, as it minimally occludes each frame, enabling the video model to better comprehend motions in the scene. Each video in the dataset captures the drumstick strokes; the audio is recorded with a shotgun microphone attached to the camera, and then denoised. The dataset provides metadata associated to each video. We use it to define textual prompts according

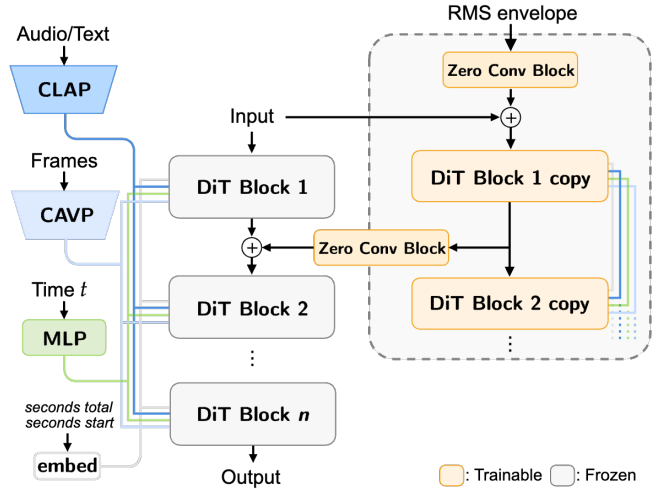


Fig. 5. Block diagram for Stable-Foley. Trainable modules are ControlNet blocks while Stable DiT blocks are frozen.

to a predetermined structure: “A person  $\{action\}$   $\{frequency\}$  on  $\{material\}$  with a wooden stick”, where  $\{action\}$  – which can be “hit” or “scratch” –,  $\{frequency\}$  – which can be either “multiple times” or “once” – and  $\{material\}$  are derived from the metadata.

The high quality of the samples in this dataset is critical for training V2A models, as very often datasets of video in the wild do not guarantee either good video and audio quality and sufficient audiovisual alignment to allow the models to learn the relationships required to generate audio that is semantically and temporally aligned with the reference video. Altogether, the dataset consists of 977 videos captured both outdoor and indoor. Indoor scenes contain a variety of hard and soft materials, such as metal, plastic, cloth, while the outdoor scenes contain materials that scatter and deform, such as grass, leaves and water. On average, each video contains 48 actions, divided between hitting and scratching. This ensures that each extracted chunk of video, lasting either 10s, contains a sufficient number of hits. We divide the dataset into 732 videos for the training set, 49 for the validation set and 196 for the test set.

2) *Walking The Maps*: We want to test our model on a case study of interest, among the most common in the sound design of audiovisual works: the generation of footsteps sounds. Datasets properly adapted for V2A tasks do not exist or are not currently publicly available. A dataset for V2A models must consist of high-resolution video and sound design-quality audio.

We therefore decided to build a small dataset with these characteristics in order to test our model in real-world scenarios for Foley synthesis. The audio and video quality of the most modern video games is extremely high, making them the perfect source, in our opinion, to create a V2A dataset. Therefore, we collected clips taken from publicly available YouTube videos of walkthroughs of some famous video games.

A lot of gamers upload videos to YouTube in which they wander around with their animated character in the maps of

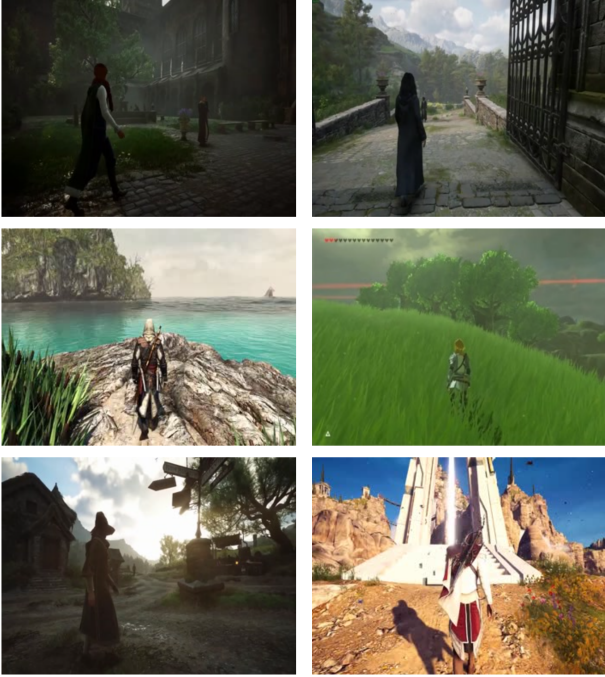


Fig. 6. Samples from the *Walking The Maps* dataset highlighting different lighting conditions and grounds.

different video games. These videos are the perfect target for our dataset, in fact the sound of footsteps is clearly audible in many cases and each footstep is strongly characterized, e.g. steps on grass, concrete or wood sound very different from each other as well as steps related to a slow walk or a run. High-definition video is associated with such sounds for more modern video games, allowing for an excellent temporal and semantic relationship between audio and video.

In order to create a first small version of our dataset, called *Walking The Maps*, we chose 4 video games as targets: *Hogwarts Legacy*, *Zelda Breath of the Wild*, *Assassin’s Creed: Odyssey*, *Assassin’s Creed IV Black Flag*. For each selected video, we extracted only clips in which the sound of the steps is clearly audible and there are no other possible sound sources in the video that can be related to the target sound.

Thus, our dataset is finally composed of 893 video clips of different lengths. The average duration of the videos is 8.82 seconds, where the shortest video has a duration of 2.04 seconds and the longest one is 72.05 seconds long. Each chunk is saved by reporting the unique ID of the video posted on YouTube, the start second of the chunk related to the full video, and the end instant expressed in seconds, so each video in the dataset will have a name of the type ID\_start\_end.mp4. The audio related to each video was subsequently preprocessed with the AudioSep [74] model using the textual query “footstep sounds” in order to separate as much as possible the footstep sound from any other noise, obtaining as clean a target audio as possible.

Since the shortest video in our dataset is 2 seconds long and our intent is mostly demonstrative, we fine-tuned our Stable-V2A model on 2 seconds chunks of each video in the dataset.

The dataset is made publicly available so that it can be used for evaluation of V2A models and to be further extended.

Some samples from our dataset are provided in Fig. 6

## B. Training and Inference Details

We train RMS-Mapper and Stable-Foley separately. The Stage 1 model is trained on a single 48 GB Nvidia RTX A6000. We use a batch size of 64, training the model for 500 epochs with a learning rate maintained constant at  $1 \times 10^{-3}$  and Adam as an optimizer with a weight decay set to  $1 \times 10^{-3}$ .

To train Stable-Foley, we use the official Stable Audio Open<sup>3</sup> repository and the related checkpoint<sup>4</sup> to initialize the weights of our model. We use 44.1 kHz stereo audio as ground truth for experiments with *Greatest Hits*. Stable-Foley is trained on a single 48 GB Nvidia RTX A6000 with a batch size of 12 for 20k steps. We use a fixed learning rate of  $1 \times 10^{-4}$  and AdamW as an optimizer, with parameters set as it is done in Stable Audio Open.

In inference, we use the RMS envelopes predicted though the RMS-Mapper, and after  $\mu$ -law decoding<sup>5</sup>, we use interpolation to match the sample rate and employ them as input to the ControlNet of Stable-Foley. The audio synthesis model, then, takes 150 sampling steps to generate the final output, using classifier-free guidance [75] with a scale set to 2.

Regarding the experiments on our *Walking The Maps* dataset, we fine-tuned our model starting from the best checkpoints obtained after training on *Greatest Hits* for both RMS-Mapper and Stable-Foley. In order to select chunks with as little background noise and camera movements as possible, we extracted 2 seconds non-overlapping chunks from each video. This implies a change in the temporal dimensions of the data in our model. Other than that, the parameters used for these experiments are the same as those used for *Greatest Hits*.

In this case, RMS-Mapper is fine-tuned with a decreasing learning rate scheduler, with  $\gamma = 0.5$ , for 2500 epochs. While Stable-Foley is fine-tuned without any change with respect to *Greatest Hits* experiments.

## C. Evaluation Metrics

To perform an objective evaluation of our model, we employ some of the most widely used metrics to attest semantic quality and time alignment in V2A tasks:

1) *E-L1*: time alignment is evaluated with the **E-L1** metric introduced in T-Foley [31]. E-L1 evaluates the fitting of the generated sounds to the temporal condition of the event:

$$E-L1 = \frac{1}{k} \sum_{i=1}^k \|\mathbf{r}_i - \hat{\mathbf{r}}_i\|, \quad (11)$$

where  $\mathbf{r}_i$  is the ground-truth envelope of the  $i$ -th frame, and  $\hat{\mathbf{r}}_i$  is the predicted one.

<sup>3</sup><https://github.com/Stability-AI/stable-audio-tools>

<sup>4</sup><https://huggingface.co/stabilityai/stable-audio-open-1.0>

<sup>5</sup>[https://librosa.org/doc/main/generated/librosa.mu\\_expand.html](https://librosa.org/doc/main/generated/librosa.mu_expand.html)



TABLE I

RESULTS FOR STABLE-V2A AND COMPARISON WITH OTHER SOTA MODELS ON *Greatest Hits*. TABLE SHOWS WHETHER THE MODEL GENERATES THE OUTPUT CONDITIONED ON AN AUDIO OR TEXT PROMPT; HRC STANDS FOR HUMAN READABLE CONTROL AND REFERS TO THE USE OF TIME-VARYING INTERPRETABLE SIGNALS THAT SOUND DESIGNERS CAN USE TO CONTROL THE GENERATION PROCESS (I.E., ENVELOPE OR ONSETS). OUR MODEL PROVIDES THE BEST RESULTS, EVEN IN THE SETTING OF TEXT CONDITIONED GENERATION.

Model	Audio	Text	HRC	FAD-P ↓	FAD-C ↓	FAD-LC ↓	E-L1 ↓	CLAP ↑	FAVD ↓
SpecVQGAN [49]	✗	✗	✗	99.07	1001	0.7102	0.0427	0.1418	6.5136
Diff-Foley [51]	✗	✗	✗	85.70	654	0.469	0.0448	0.3733	4.6186
CondFoleyGen [50]	✓	✗	✗	74.93	650	0.4883	0.0357	0.4879	6.4814
SyncFusion [30]	✗	✓	✓	35.64	591	0.4365	0.0231	0.5154	4.3020
	✓	✗	✓	27.85	542	0.2793	0.0177	0.6621	3.2825
Video-Foley [54]	✗	✓	✓	67.04	644	0.4997	0.0242	0.3680	4.9106
	✓	✗	✓	28.45	435	0.1671	0.0183	0.6779	2.2070
Stable-V2A (Ours)	✗	✓	✓	32.80	381	0.2516	<b>0.0137</b>	0.4806	3.9413
	✓	✗	✓	<b>16.57</b>	<b>217</b>	<b>0.1048</b>	<b>0.0137</b>	<b>0.6833</b>	<b>2.0264</b>

2) *Accuracy metric*: we also use **class-wise accuracy** at  $k$  ( $k = \{1, 5, 10\}$ ). Since we are not trying to make a perfect classification of the various frames in the envelope, as we do not want to penalize near-correct predictions, the most informative accuracy is  $\text{acc}@5$ .

3) *Fréchet Audio Distance*: **FAD** [76] is used to evaluate the quality and realism of generated audio compared to reference audio. This metric computes the similarity between the statistical distributions of embeddings of the real and generated audio.

The choice of audio encoder from which to extract embeddings significantly impacts the FAD score because different features representations encode specific aspects of audio, so the audio quality measured by this metric with respect to human perception is embeddings dependent. For this reason we measure FAD using three different audio encoders: PANNs wavegram-logmel [77] (**FAD-P**), Microsoft CLAP [78] (**FAD-C**) and Laion-CLAP [35] (**FAD-LC**).

To calculate these metrics, we use the *fadtk*<sup>6</sup> library.

4) *CLAP-score metric*: **CLAP-score** is another metric used to assess the overall quality of the generated waveforms, as done in [33]. We generate embeddings through CLAP [35] of both ground truth and generated audio and compute cosine similarity between them. Since our model is based on the use of CLAP as the audio representation, this metric is useful for attesting how relevant the conditioning audio features are in generating the final output.

5) *Fréchet Audio-Visual Distance*: **FAVD** [79] is gaining increasing popularity in the evaluation of V2A models, as the purpose of this metric is to measure the temporal and semantic alignment between video and audio modalities. It does so by calculating the Fréchet Distance between video embedding and audio embedding. In our case, we use video and audio encoders used in the reference library, namely I3D [80] and VGGish [81], to calculate the embedding of the ground truth video and the embedding of the generated audio.

We use E-L1,  $\text{acc}@1$ ,  $\text{acc}@5$ ,  $\text{acc}@10$  for the evaluation of the RMS-Mapper, while we use FAD-P, FAD-C, FAD-LC, CLAP-score, FAVD and E-L1 for the evaluation of both Stable-Foley and the complete model, Stable-V2A.

## VI. RESULTS

### A. Complete Model

We compare our complete model, Stable-V2A, with the main V2A models publicly available at the time of writing this paper. More precisely, our baseline models are the aforementioned SpecVQGAN [49], CondFoleyGen [50], Diff-Foley [51], Video-Foley [54] and SyncFusion [30].

For all available models, we use the official code provided on GitHub along with their checkpoints. For comparison with [54], we used our video model to generate the RMS envelopes, as at the time of writing this paper the only code and checkpoints available are for the audio synthesis model.

As shown in Table I, Stable-V2A achieves improved results across all metrics, including both time alignment and the semantic quality of the generated audio, compared to all baseline models considered. These results highlight the importance of using a strong temporal control, such as the envelope, to guide the generation of audio. Indeed, the second- and third-best models in our tests, Video-Foley and SyncFusion, use envelope and onset tracks for temporal conditioning, providing a stronger guide for temporal alignment than the methods employed by SpecVQGAN, CondFoleyGen, and Diff-Foley.

Furthermore, the results on audio quality metrics demonstrate the critical importance of leveraging a state-of-the-art model like Stable Audio for audio generation. Achieving high audio definition in V2A models is crucial to making these tools actually useful for sound designers.

The use of ControlNet enables us to leverage the prior knowledge of Stable Audio for generating ambient sounds, allowing the production of 44.1 kHz stereo audio effects, matching professional audio production standards. Additionally, the integration of ControlNet with a high depth\_factor of 20% ensures that our model is both lightweight and fast. In fact, the results we achieve are based on training Stable-Foley on a small dataset of approximately 6 hours, such as *Greatest Hits*, with a limited number of training steps, thus avoiding the need for substantial time and computational resources.

Table IV shows the results on objective metrics obtained by evaluating our model on the Walking The Maps test set. Both the video model and the audio model, succeed to obtain good results for the synchronization between audio and video as

<sup>6</sup><https://github.com/DCASE2024-Task7-Sound-Scene-Synthesis/fadtk>

TABLE II  
RESULTS FOR RMS-MAPPER WITH DIFFERENT RGB AND OPT. FLOW ENCODERS.

Encoder	RGB	Opt. Flow	E-L1 ↓	Acc@1 ↑	Acc@5 ↑	Acc@10 ↑
BN-Inception	✓	✓	0.01	0.092	0.398	0.630
TC-CLIP	✓	✗	0.0130	0.073	0.340	0.536
TC-CLIP	✓	✓	<b>0.0115</b>	<b>0.104</b>	<b>0.430</b>	<b>0.650</b>

TABLE III  
RESULTS FOR STABLE-FOLEY FOR AUDIO PROMPT AND GROUND-TRUTH RMS WITH AND WITHOUT FRAMES CONDITIONING.

Model	Frames Cond.	FAD-P ↓	FAD-C ↓	FAD-LC ↓	E-L1 ↓	CLAP ↑	FAVD ↓
GT RMS	✗	9.0722	<b>252</b>	0.0635	0.0062	0.7640	1.7103
	✓	<b>7.67</b>	260	<b>0.0630</b>	<b>0.0060</b>	<b>0.7762</b>	<b>1.5832</b>

TABLE IV  
RESULTS FOR STABLE-V2A ON *Walking The Maps*.

Model	FAD-C ↑	FAD-LC ↑	E-L1 ↑	CLAP ↑	FAVD ↓
Stable-V2A	167	0.2556	0.0460	0.6956	3.0682

well as for the quality of the produced waveforms, managing to generate realistic footsteps sounds. The sounds produced are diversified from each other according to both the type of walking of the animated character and the type of ground on which that character walks.

### B. Ablation studies

1) *RMS-Mapper*: our experiments demonstrate the fundamental importance of the optical flow information. When we provide the model with only the features derived from video frames, the results are significantly worse compared to using the concatenation of RGB and optical flow features.

We also experiment with the feature extractor used in RegNet, that is BN-Inception [82]. This network is trained on images, so the features extracted for one frame are not correlated with those of other frames. However, it is trained on an extremely large dataset (ImageNet [83]), allowing it to generalize well and produce strong results even when encoding video frames, despite not being designed for this purpose. Our experiments show that TC-CLIP achieves better results than BN-Inception, although by a limited margin. This outcome is significant, as TC-CLIP is trained on a smaller dataset (Kinetics-400 [84]) specifically designed for motion recognition. In our opinion, this demonstrates the direction V2A research should pursue: employing models specifically designed to capture temporal context.

Results for RMS-Mapper and relative ablation studies are reported in Table II.

2) *Stable-Foley*: we evaluate Stable-Foley by generating audio through ground truth RMS envelopes extracted directly from waveforms. As ablation study, we train the model without the direct conditioning of frames provided by CAVP. The results reported in Table III show that such additional information leads to a perceptible improvement in the semantics of the produced audio, as can be noticed from the metrics for semantic alignment. While there is no perceivable enhancement in temporal alignment; this result shows that temporal

conditioning is contributed entirely by the ControlNet input, demonstrating the strength of such conditioning, which is the desired result.

## VII. CONCLUSION AND DISCUSSION

In this paper, we present a model for generating an audio track semantically and temporally aligned to a silent input video, called Stable-V2A. The model is divided into two distinct parts, trained separately and joined only at inference time: RMS-Mapper, which maps a representative envelope of the audio to be generated directly from the reference video, and Stable-Foley, a sound synthesis model that, through the use of the predicted envelope and other semantic controls, generates the final output of the model. Our sound synthesis model is based on Stable Audio Open and, to the best of our knowledge, this is the first time that such a state-of-the-art model for audio generation is used in the context of Video-to-Audio.

Although the audio synthesis model tracks with high accuracy the envelope used as a control, mapping that envelope from the video represents the bottleneck of our model, still leaving room for many potential research works.

In addition, datasets suitable for V2A problems, containing high-quality video and audio, are still too few or difficult to obtain. In our case, we believe that the introduction of suitable datasets, such as *Walking The Maps*, can be of great help for researchers in the field of Foley synthesis.

Also, the semantics of the generated waveforms can be further optimized through the use of different and more relevant semantic conditionings.

## VIII. ACKNOWLEDGEMENTS

This work was supported by the European Union under the Italian National Recovery and Resilience Plan (NRRP) of NextGenerationEU, partnership on “National Centre for HPC, Big Data and Quantum Computing” (CN00000013 - Spoke 6: Multiscale Modelling & Engineering Applications).

This work was supported by “Progetti di Ricerca Medi” of Sapienza University of Rome for the project “SAID: Solving Audio Inverse problems with Diffusion models”, under grant number RM123188F75F8072.

E.P. and L.C. were partially supported by PRIN 2022 project no. 2022AL45R2 (EYE-FLAI, CUP H53D2300350-0001).

M. C. was funded by UKRI and EPSRC as part of the “UKRI CDT in Artificial Intelligence and Music”, under grant EP/S022694/1.

## REFERENCES

- [1] M. Suzuki and Y. Matsuo, “A survey of multimodal deep generative models,” *Advanced Robotics*, vol. 36, pp. 261 – 278, 2022.
- [2] E. Guizzo, R. F. Gramaccioni, S. Jamili, C. Marinoni, E. Massaro, C. Medaglia, G. Nachira, L. Nucciarelli, L. Paglialunga, M. Pennese, S. Pepe, E. Rocchi, A. Uncini, and D. Comminiello, “L3DAS21 challenge: Machine learning for 3D audio signal processing,” in *IEEE 31st International Workshop on Machine Learning for Signal Processing (MLSP)*, 2021, pp. 1–6.
- [3] E. Guizzo, C. Marinoni, M. Pennese, X. Ren, X. Zheng, C. Zhang, B. S. Masiero, A. Uncini, and D. Comminiello, “L3DAS22 challenge: Learning 3D audio sources in a real office environment,” in *IEEE International Conference on Acoustics, Speech and Signal Processing (ICASSP)*, 2022, pp. 9186–9190.
- [4] H. Zhang, X. Li, and L. Bing, “Video-LLaMA: An instruction-tuned audio-visual language model for video understanding,” in *Conference on Empirical Methods in Natural Language Processing: System Demonstrations (EMNLP)*, 2023, pp. 543–553.
- [5] Y. Tang, D. Shimada, J. Bi, M. Feng, H. Hua, and C. Xu, “Empowering llms with pseudo-untrimmed videos for audio-visual temporal understanding,” *arXiv preprint arXiv:2403.16276*, 2024.
- [6] H. Liu, Z. Chen, Y. Yuan, X. Mei, X. Liu, D. Mandic, W. Wang, and M. D. Plumbley, “AudioLDM: Text-to-audio generation with latent diffusion models,” in *International Conference on Machine Learning (ICML)*, vol. 202, 2023, pp. 21 450–21 474.
- [7] R. Huang, J. Huang, D. Yang, Y. Ren, L. Liu, M. Li, Z. Ye, J. Liu, X. Yin, and Z. Zhao, “Make-an-audio: Text-to-audio generation with prompt-enhanced diffusion models,” in *International Conference on Machine Learning (ICML)*, vol. 202, 2023, pp. 13 916–13 932.
- [8] R. Liu, Y. Hu, H. Zuo, Z. Luo, L. Wang, and G. Gao, “Text-to-speech for low-resource agglutinative language with morphology-aware language model pre-training,” *IEEE/ACM Transactions on Audio, Speech, and Language Processing*, vol. 32, pp. 1075–1087, 2024.
- [9] Y. Yuan, H. Liu, X. Liu, Q. Huang, M. . Plumbley, and W. Wang, “Retrieval-augmented text-to-audio generation,” in *IEEE International Conference on Acoustics, Speech and Signal Processing (ICASSP)*, 2023, pp. 581–585.
- [10] M. Comunità, Z. Zhong, A. Takahashi, S. Yang, M. Zhao, K. Saito, Y. Ikemiya, T. Shibuya, S. Takahashi, and Y. Mitsufuji, “Specmaskgit: Masked generative modeling of audio spectrograms for efficient audio synthesis and beyond,” *arXiv preprint arXiv:2406.17672*, 2024.
- [11] Y. Aytar, C. Vondrick, and A. Torralba, “Soundnet: Learning sound representations from unlabeled video,” in *Advances in Neural Information Processing Systems (NeurIPS)*, 2016, p. 892–900.
- [12] Y. Zhou, Z. Wang, C. Fang, T. Bui, and T. L. Berg, “Visual to sound: Generating natural sound for videos in the wild,” in *IEEE/CVF Conference on Computer Vision and Pattern Recognition (CVPR)*, 2018, pp. 3550–3558.
- [13] R. Sheffer and Y. Adi, “I hear your true colors: Image guided audio generation,” in *IEEE International Conference on Acoustics, Speech and Signal Processing (ICASSP)*, 2023, pp. 1–5.
- [14] S. Ghose and J. J. Prevost, “AutoFoley: Artificial synthesis of synchronized sound tracks for silent videos with deep learning,” *IEEE Transactions on Multimedia*, vol. 23, pp. 1895–1907, 2021.
- [15] S. Ghose and J. J. Prevost, “FoleyGAN: Visually guided generative adversarial network-based synchronous sound generation in silent videos,” *IEEE Transactions on Multimedia*, vol. 25, pp. 4508–4519, 2023.
- [16] Z. Chen, D. Geng, and A. Owens, “Images that sound: Composing images and sounds on a single canvas,” in *Advances in Neural Information Processing Systems (NeurIPS)*, 2024.
- [17] R. F. Gramaccioni, C. Marinoni, C. Chen, A. Uncini, and D. Comminiello, “L3DAS23: Learning 3d audio sources for audio-visual extended reality,” *IEEE Open Journal of Signal Processing*, vol. 5, pp. 632–640, 2024.
- [18] V. Dassani, J. Bird, and D. Cliff, “Automated composition of picture-synched music soundtracks for movies,” in *Proceedings of the 16th ACM SIGGRAPH European Conference on Visual Media Production*, 2019.
- [19] S. Di, Z. Jiang, S. Liu, Z. Wang, L. Zhu, Z. He, H. Liu, and S. Yan, “Video background music generation with controllable music transformer,” in *ACM Multimedia*, 2021, p. 2037–2045.
- [20] L. Zhuo, Z. Wang, B. Wang, Y. Liao, C. Bao, S. Peng, S. Han, A. Zhang, F. Fang, and S. Liu, “Video background music generation: Dataset, method and evaluation,” in *Proceedings of the IEEE/CVF International Conference on Computer Vision (ICCV)*, 2023, pp. 15 637–15 647.
- [21] G. Chen, G. Wang, X. Huang, and J. Sang, “Semantically consistent video-to-audio generation using multimodal language large model,” *arXiv preprint arXiv:2404.16305*, 2024.
- [22] H. Gao, “An overview of visual sound synthesis generation tasks based on deep learning networks,” *Transactions on Engineering and Technology Research*, vol. 13, 2023.
- [23] M. Keetels and J. Vroomen, “Perception of synchrony between the senses,” *The neural bases of multisensory processes*, pp. 147–177, 2012.
- [24] K. Chen, C. Zhang, C. Fang, Z. Wang, T. Bui, and R. Nevatia, “Visually indicated sound generation by perceptually optimized classification,” in *ECCV Workshops*, 2018.
- [25] C. Cui, Y. Ren, J. Liu, R. Huang, and Z. Zhao, “Varietysound: Timbre-controllable video to sound generation via unsupervised information disentanglement,” in *IEEE International Conference on Acoustics, Speech and Signal Processing (ICASSP)*, 2023, pp. 1–5.
- [26] M. Yi and M. Li, “Efficient video to audio mapper with visual scene detection,” *ArXiv*, vol. abs/2409.09823, 2024.
- [27] M. Ishii, A. Hayakawa, T. Shibuya, and Y. Mitsufuji, “A simple but strong baseline for sounding video generation: Effective adaptation of audio and video diffusion models for joint generation,” *arXiv preprint arXiv:2409.17550*, 2024.
- [28] Y. Ren, C. Li, M. Xu, W. Liang, Y. Gu, R. Chen, and D. Yu, “STA-V2A: Video-to-audio generation with semantic and temporal alignment,” *arXiv preprint arXiv:2409.08601*, 2024.
- [29] Y. Jeong, Y. Kim, S. Chun, and J. Lee, “Read, watch and scream! sound generation from text and video,” *arXiv preprint arXiv:2407.05551*, 2024.
- [30] M. Comunità, R. F. Gramaccioni, E. Postolache, E. Rodolà, D. Comminiello, and J. D. Reiss, “Synfusion: Multimodal onset-synchronized video-to-audio foley synthesis,” in *IEEE International Conference on Acoustics, Speech and Signal Processing (ICASSP)*, 2024, pp. 936–940.
- [31] Y. Chung, J. Lee, and J. Nam, “T-foley: A controllable waveform-domain diffusion model for temporal-event-guided foley sound synthesis,” in *IEEE International Conference on Acoustics, Speech and Signal Processing (ICASSP)*, 2024, pp. 6820–6824.
- [32] P. Chen, Y. Zhang, M. Tan, H. Xiao, D. Huang, and C. Gan, “Generating visually aligned sound from videos,” *IEEE Transactions on Image Processing*, vol. 29, pp. 8292–8302, 2020.
- [33] Z. Evans, J. Parker, C. Carr, Z. Zukowski, J. Taylor, and J. Pons, “Stable audio open,” *arXiv preprint arXiv:2407.14358*, 2024.
- [34] L. Zhang, A. Rao, and M. Agrawala, “Adding conditional control to text-to-image diffusion models,” in *IEEE International Conference on Computer Vision (ICCV)*, 2023, pp. 3813–3824.
- [35] Y. Wu\*, K. Chen\*, T. Zhang\*, Y. Hui\*, T. Berg-Kirkpatrick, and S. Dubnov, “Large-scale contrastive language-audio pretraining with feature fusion and keyword-to-caption augmentation,” in *IEEE International Conference on Acoustics, Speech and Signal Processing (ICASSP)*, 2023, pp. 1–5.
- [36] A. Owens, P. Isola, J. H. McDermott, A. Torralba, E. H. Adelson, and W. T. Freeman, “Visually indicated sounds,” in *IEEE Conference on Computer Vision and Pattern Recognition (CVPR)*, 2016, pp. 2405–2413.
- [37] M. Comunità, H. Phan, and J. D. Reiss, “Neural synthesis of footsteps sound effects with generative adversarial networks,” in *Audio Engineering Society Convention*, 2022.
- [38] D. Ceylan, C.-H. P. Huang, and N. J. Mitra, “Pix2Video: Video editing using image diffusion,” in *IEEE/CVF International Conference on Computer Vision (ICCV)*, 2023, pp. 23 149–23 160.
- [39] S. Jenni, A. Black, and J. P. Collomosse, “Audio-visual contrastive learning with temporal self-supervision,” in *AAAI Conference on Artificial Intelligence*, 2023.
- [40] D. Fedorishin, L. Lu, S. Setlur, and V. Govindaraju, “Audio match cutting: Finding and creating matching audio transitions in movies and

- videos,” in *IEEE International Conference on Acoustics, Speech and Signal Processing (ICASSP)*, 2024, pp. 6200–6204.
- [41] N. Sahipjohn, A. Gudmalwar, N. Shah, P. Wasnik, and R. R. Shah, “DubWise: Video-guided speech duration control in multimodal llm-based text-to-speech for dubbing,” in *Interspeech*, 2024, pp. 2960–2964.
- [42] M. F. Colombo, F. Ronchini, L. Comanducci, and F. Antonacci, “MambaFoley: Foley sound generation using selective state-space models,” *arXiv preprint arXiv:2409.09162*, 2024.
- [43] X. Liu, T. Iqbal, J. Zhao, Q. Huang, M. D. Plumbley, and W. Wang, “Conditional sound generation using neural discrete time-frequency representation learning,” in *IEEE 31st International Workshop on Machine Learning for Signal Processing (MLSP)*, 2021, pp. 1–6.
- [44] Y. Yuan, H. Liu, X. Liu, X. Kang, M. D. Plumbley, and W. Wang, “Latent diffusion model based foley sound generation system for dease challenge 2023 task 7,” *arXiv preprint arXiv:2305.15905*, 2023.
- [45] J. Lee and J. D. Reiss, “Real-time sound synthesis of audience applause,” *Journal of the Audio Engineering Society*, 2020.
- [46] A. Radford, J. W. Kim, C. Hallacy, A. Ramesh, G. Goh, S. Agarwal, G. Sastry, A. Askell, P. Mishkin, J. Clark, G. Krueger, and I. Sutskever, “Learning transferable visual models from natural language supervision,” in *International Conference on Machine Learning (ICML)*, vol. 139, 2021, pp. 8748–8763.
- [47] Y. Xing, Y.-Y. He, Z. Tian, X. Wang, and Q. Chen, “Seeing and Hearing: Open-domain visual-audio generation with diffusion latent aligners,” in *IEEE/CVF Conference on Computer Vision and Pattern Recognition (CVPR)*, 2024, pp. 7151–7161.
- [48] R. Girdhar, A. El-Nouby, Z. Liu, M. Singh, K. V. Alwala, A. Joulin, and I. Misra, “ImageBind one embedding space to bind them all,” in *IEEE/CVF Conference on Computer Vision and Pattern Recognition (CVPR)*, 2023, pp. 15 180–15 190.
- [49] V. Iashin and E. Rahtu, “Taming visually guided sound generation,” in *British Machine Vision Conference (BMVC)*, 2021.
- [50] Y. Du, Z. Chen, J. Salamon, B. Russell, and A. Owens, “Conditional generation of audio from video via foley analogies,” in *Conference on Computer Vision and Pattern Recognition (CVPR)*, 2023, pp. 2426–2436.
- [51] S. Luo, C. Yan, C. Hu, and H. Zhao, “Diff-Foley: Synchronized video-to-audio synthesis with latent diffusion models,” in *Advances in Neural Information Processing Systems (NeurIPS)*, vol. 36, 2023, pp. 48 855–48 876.
- [52] D. Tran, H. Wang, L. Torresani, J. Ray, Y. LeCun, and M. Paluri, “A closer look at spatiotemporal convolutions for action recognition,” in *IEEE/CVF Conference on Computer Vision and Pattern Recognition (CVPR)*, 2018, pp. 6450–6459.
- [53] F. Schneider, O. Kamal, Z. Jin, and B. Schölkopf, “Mousai: Text-to-music generation with long-context latent diffusion,” *arXiv preprint arXiv:2301.11757*, 2023.
- [54] J. Lee, J.-Y. Im, D. Kim, and J. Nam, “Video-Foley: Two-stage video-to-sound generation via temporal event condition for foley sound,” *arXiv preprint arXiv:2408.11915*, 2024.
- [55] J. Ho, A. Jain, and P. Abbeel, “Denosing diffusion probabilistic models,” in *Advances in Neural Information Processing Systems (NeurIPS)*, vol. 33, 2020, pp. 6840–6851.
- [56] G. Mariani, I. Tallini, E. Postolache, M. Mancusi, L. Cosmo, and E. Rodolà, “Multi-source diffusion models for simultaneous music generation and separation,” in *International Conference on Learning Representations (ICLR)*, 2024.
- [57] Z. Kong, W. Ping, J. Huang, K. Zhao, and B. Catanzaro, “DiffWave: A versatile diffusion model for audio synthesis,” in *International Conference on Learning Representations (ICLR)*, 2021.
- [58] R. Rombach, A. Blattmann, D. Lorenz, P. Esser, and B. Ommer, “High-resolution image synthesis with latent diffusion models,” in *IEEE/CVF Conference on Computer Vision and Pattern Recognition (CVPR)*, 2022, pp. 10 674–10 685.
- [59] H. Liu, Q. Tian, Y. Yuan, X. Liu, X. Mei, Q. Kong, Y. Wang, W. Wang, Y. Wang, and M. D. Plumbley, “AudioLDM 2: Learning holistic audio generation with self-supervised pretraining,” *IEEE/ACM Transactions on Audio, Speech, and Language Processing*, vol. 32, pp. 2871–2883, 2023.
- [60] Z. Evans, C. Carr, J. Taylor, S. H. Hawley, and J. Pons, “Fast timing-conditioned latent audio diffusion,” *arXiv preprint arXiv:2402.04825*, 2024.
- [61] Z. Evans, J. Parker, C. Carr, Z. Zukowski, J. Taylor, and J. Pons, “Long-form music generation with latent diffusion,” *arXiv preprint arXiv:2404.10301*, 2024.
- [62] J. Chen, J. YU, C. GE, L. Yao, E. Xie, Z. Wang, J. Kwok, P. Luo, H. Lu, and Z. Li, “PixArt- $\alpha$ : Fast training of diffusion transformer for photorealistic text-to-image synthesis,” in *International Conference on Learning Representations (ICLR)*, 2024.
- [63] S.-L. Wu, C. Donahue, S. Watanabe, and N. J. Bryan, “Music Control-Net: Multiple time-varying controls for music generation,” *IEEE/ACM Transactions on Audio, Speech, and Language Processing*, vol. 32, pp. 2692–2703, 2023.
- [64] N. Garcia-Sihua, Y. Zong, and J. Reiss, “Discerning real from synthetic: analysis and perceptual evaluation of sound effects,” in *Audio Engineering Society Conference*, 2024.
- [65] zong yisu, garcia-sihua nelly, and reiss joshua, “a machine learning method to evaluate and improve sound effects synthesis model design,” *Journal of the Audio Engineering Society*, 2024.
- [66] A. van den Oord, S. Dieleman, H. Zen, K. Simonyan, O. Vinyals, A. Graves, N. Kalchbrenner, A. W. Senior, and K. Kavukcuoglu, “WaveNet: A generative model for raw audio,” in *Speech Synthesis Workshop*, 2016.
- [67] S. Kum and J. Nam, “Joint detection and classification of singing voice melody using convolutional recurrent neural networks,” *Applied Sciences*, 2019.
- [68] Z. Teed and J. Deng, “RAFT: Recurrent all-pairs field transforms for optical flow,” in *European Conference on Computer Vision (ECCV)*, 2020, pp. 402–419.
- [69] M. Kim, D. Han, T. Kim, and B. Han, “Leveraging temporal contextualization for video action recognition,” in *European Conference on Computer Vision (ECCV)*, 2024, pp. 74–91.
- [70] A. Graves and J. Schmidhuber, “Framewise phoneme classification with bidirectional LSTM networks,” in *IEEE International Joint Conference on Neural Networks (IJCNN)*, vol. 4, 2005, pp. 2047–2052 vol. 4.
- [71] C. J. Steinmetz and J. D. Reiss, “auraloss: Audio focused loss functions in PyTorch,” in *Digital Music Research Network One-day Workshop (DMRN+15)*, 2020.
- [72] A. Défossez, J. Copet, G. Synnaeve, and Y. Adi, “High fidelity neural audio compression,” *Transactions on Machine Learning Research*, 2023.
- [73] D. Niizumi, D. Takeuchi, Y. Ohishi, N. Harada, and K. Kashino, “BYOL for Audio: Self-supervised learning for general-purpose audio representation,” in *International Joint Conference on Neural Networks (IJCNN)*, 2021, pp. 1–8.
- [74] X. Liu, H. Liu, Q. Kong, X. Mei, J. Zhao, Q. Huang, M. D. Plumbley, and W. Wang, “Separate What You Describe: Language-queried audio source separation,” in *Interspeech*, 2022, pp. 1801–1805.
- [75] J. Ho and T. Salimans, “Classifier-free diffusion guidance,” in *NeurIPS Workshop on Deep Generative Models and Downstream Applications*, 2021.
- [76] K. Kilgour, M. Zuluaga, D. Roblek, and M. Sharifi, “Fréchet audio distance: A reference-free metric for evaluating music enhancement algorithms,” in *Interspeech*, 2019, pp. 2350–2354.
- [77] Q. Kong, Y. Cao, T. Iqbal, Y. Wang, W. Wang, and M. D. Plumbley, “PANNs: Large-scale pretrained audio neural networks for audio pattern recognition,” *IEEE/ACM Transactions on Audio, Speech, and Language Processing*, vol. 28, pp. 2880–2894, 2019.
- [78] B. Elizalde, S. Deshmukh, M. A. Ismail, and H. Wang, “CLAP learning audio concepts from natural language supervision,” in *IEEE International Conference on Acoustics, Speech and Signal Processing (ICASSP)*, 2023, pp. 1–5.
- [79] L. Goncalves, P. Mathur, C. Lavania, M. Cekic, M. Federico, and K. J. Han, “Perceptual evaluation of audio-visual synchrony grounded in viewers’ opinion scores,” in *European Conference on Computer Vision (ECCV)*. Cham: Springer Nature Switzerland, 2024, pp. 288–305.
- [80] J. Carreira and A. Zisserman, “Quo vadis, action recognition? a new model and the kinetics dataset,” in *IEEE Conference on Computer Vision and Pattern Recognition (CVPR)*, 2017, pp. 4724–4733.
- [81] S. Hershey, S. Chaudhuri, D. P. W. Ellis, J. F. Gemmeke, A. Jansen, R. C. Moore, M. Plakal, D. Platt, R. A. Saurous, B. Seybold, M. Slaney, R. J. Weiss, and K. W. Wilson, “CNN architectures for large-scale audio classification,” in *IEEE International Conference on Acoustics, Speech and Signal Processing (ICASSP)*, 2017, pp. 131–135.
- [82] S. Ioffe and C. Szegedy, “Batch normalization: accelerating deep network training by reducing internal covariate shift,” in *International Conference on Machine Learning (ICML)*, ser. ICML’15, 2015, p. 448–456.
- [83] J. Deng, W. Dong, R. Socher, L.-J. Li, K. Li, and L. Fei-Fei, “ImageNet: A large-scale hierarchical image database,” in *IEEE Conference on Computer Vision and Pattern Recognition (CVPR)*, 2009, pp. 248–255.
- [84] W. Kay, J. Carreira, K. Simonyan, B. Zhang, C. Hillier, S. Vijayanarasimhan, F. Viola, T. Green, T. Back, A. Natsev, M. Suleyman, and A. Zisserman, “The kinetics human action video dataset,” *arXiv preprint arXiv:1705.06950*, 2017.